Natural Resonance Theory: I. General Formalism

E. D. GLENDENING* AND F. WEINHOLD

Theoretical Chemistry Institute and Department of Chemistry, University of Wisconsin, Madison, Wisconsin 53706

Received 15 July 1997; accepted 1 November 1997

ABSTRACT: We present a new quantum-mechanical resonance theory based on the first-order reduced density matrix and its representation in terms of natural bond orbitals (NBOs). This ''natural'' resonance theory (NRT) departs in important respects from the classical Pauling-Wheland formulation, yet it leads to quantitative resonance weights that are in qualitative accord with conventional resonance theory and chemical intuition. The NRT variational functional leads to an optimal resonance-weighted approximation to the full density matrix, combining the ''single reference'' limit of weak delocalization (incorporating diagonal population changes only) with the full ''multireference'' limit of strong delocalization (incorporating off-diagonal couplings between resonance structures). The NRT variational functional yields an error measure that serves as an intrinsic criterion of accuracy of the resonance-theoretic description. The

* Present address: Department of Chemistry, Indiana State University, Terre Haute, IN 47809.

Correspondence to: F. Weinhold

Editor's Note: This set of three papers elicited strong objections from one respondent, which were not resolved on revision. A brief summary of this referee's criticisms and the authors' response follow.

Referee's caveat: The proposed ''natural resonance theory'' does not meet the requirements of a theoretically correct approach. As we are dealing with *pure quantum mechanical states* described by a well-defined wave function, the use of *incoherent* superposition (3.1) of localized density matrices to characterize the given system is a mistake from the conceptual point of view and cannot be justified even by appealing to ''chemically reasonable'' numerical results. (But it is also questionable whether the results are really ''chemically reasonable''; e.g., the expansion (3.1) cannot account for the significant *negative* value of the 1–4 π-density matrix element of the butadiene molecule, to which one can assign an important chemical significance.)

In quantum mechanics it is of meaning to consider expansions of the wave functions, but it is not allowed to simulate the first-order density matrix as a superposition of independent first-order density matrices of selected idealized structures. This gives a fundamental difference between the old resonance theory and the present formalism. In my opinion, the MO language is inadequate to discuss the concept of ''resonance''; it has the concept of ''delocalization'' instead.

A brief response to the referee's points: We concur (and have attempted to emphasize) that there is ''a fundamental difference between the old resonance theory and the present formalism.'' What is ''chemically reasonable'' will ultimately be judged by comparisons with experiment, not with supposed Hückel-type analogs. We do not concur that there is a fundamental distinction between ''resonance'' and ''delocalization'' (insofar as both terms express departures from a single idealized Lewis structure), nor that MO theory is somehow more adequate to discuss the latter than the former.

Journal of Computational Chemistry, Vol. 19, No. 6, 593–609 (1998)

CCC 0192-8651 / 98 / 060593-17

NRT program structure, algorithms, and numerical characteristics are described in supplementary material, and detailed chemical applications are presented in two companion papers. J Comput Chem 19: 593–609, 1998

Keywords: natural resonance theory; resonance theory; natural bond orbitals

Introduction

The theory of resonance, as Pauling remarked,[1] ''is now treated in essentially every textbook of chemistry and is used by essentially every chemist.'' However, despite its widespread usage, resonance theory[2–4] now serves primarily as a heuristic conceptual framework rather than as a quantitative theory of chemical structure and reactivity.[5] Although resonance concepts retain considerable intuitive appeal, only partial success has been achieved in formulating these concepts in modern *ab initio* terms or increasing their predictive reliability. The goal of the present work is to present a practical numerical algorithm by which the results of contemporary *ab initio* calculations can be quantitatively expressed in the language of resonance theory.

Basic resonance-theoretic premises can be illustrated with reference to the famous example of amide resonance[6] in the formamide molecule:

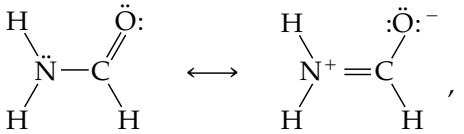

I **II**

which is pictured as having fractional bond orders and other properties *intermediate* between those of the localized structures, I and II, with relative weightings $w_{\rm I}, w_{\rm II}$ estimated[6] as 0.6 and 0.4, respectively. More generally, a molecular property $\langle P \rangle$ can be expressed as the weighted average of idealized values $\langle P \rangle_\alpha$ associated with hypothetical localized structural formulas α,

$$\langle P \rangle = \sum_\alpha w_\alpha \langle P \rangle_\alpha \qquad (1.1a)$$

with nonnegative weighting factors summing to unity

$$w_\alpha \geq 0, \qquad \sum_\alpha w_\alpha = 1. \qquad (1.1b)$$

Each A—B bond is thereby pictured as having fractional bond order[7]

$$b_{\rm AB} = \sum_\alpha w_\alpha b_{\rm AB}^{(\alpha)} \qquad (1.2)$$

intermediate between the integer values $b_{\rm AB}^{(\alpha)}$ depicted in idealized localized structures. A further premise is that resonance delocalization confers additional *stabilization* energy

$$\Delta E_\alpha \propto w_\alpha \qquad (1.3)$$

in proportion to its relative weighting. The simple resonance concepts embodied in (1.1)–(1.3) allow a far-reaching extension of classical structure theory to molecules that cannot be adequately represented by a single structural formula.[3]

Whereas formulas (1.1)–(1.3) are often associated with the quantum-mechanical resonance formalism of Pauling and Wheland (PW),[2–4] it should be noted that the basic concept of representing a molecule as an ''average'' of two or more idealized structural forms traces back at least to Kekulé's famous 1865 benzene dream.[8] Indeed, the rather parallel ''electromerism theory'' of Robinson[9] and Ingold[10] was developed essentially without reference to quantum theory.[11] Nevertheless, it was the influential PW formulation that established the concepts and nomenclature of resonance theory as presently understood by most chemists.

PW introduced a formal rationale for formulas (1.1)–(1.3) in terms of the wavefunction *ansatz*

$$\Psi = \sum_\alpha c_\alpha \Psi_\alpha \qquad (1.4a)$$

$$w_\alpha = |c_\alpha|^2 \qquad (1.4b)$$

where Ψ_α is identified as the HLSP-PP-VB (Heitler-London-Slater-Pauling perfect-pairing valence

bond)[12] approximate wave function for localized Lewis structure α. Persistent difficulties in evaluating the coefficients c_α and accounting for omitted cross-terms (see the following section) severely limited the role of rigorous *ab initio* evaluations in constraining the empirical applications of the theory. Eventually, these difficulties resulted in resonance-type rationalizations being largely supplanted by corresponding MO-based descriptions in which ''resonance weights'' play no direct role. Despite the relative neglect of the resonance-theoretic framework for quantitative *ab initio* purposes, the concepts of resonance theory continue to exert profound influence on the theory and practice of chemistry.[13]

In the present work we present an alternative formulation of resonance theory that avoids difficulties of the PW *ansatz* (1.4) yet retains the spirit of older electromerism/resonance theories and leads to practical evaluation of expressions such as (1.2) by rigorous *ab initio* means. Our approach is based on the formal properties of the first-order reduced density matrix[14] in the natural bond orbital (NBO)[15] representation and is referred to as *natural resonance theory* (NRT) to distinguish it from earlier formulations.

The plan of the paper is as follows: We briefly summarize formal difficulties of the PW formalism and outline the alternative density matrix formulation of resonance weighting. This leads to presentation of the general NRT algorithm, including formation of candidate resonance structures and the NRT variational functionals for ''single reference'' and multireference cases. Further details of the NRT optimization procedure (see also supplementary material) are followed by a discussion. Numerical NRT applications to chemical systems are presented in the two companion papers.

Pauling-Wheland Resonance Theory

As was stated above, the resonance-averaging concepts summarized in (1.1)–(1.3) can be expressed without reference to wave functions, but PW introduced specific quantum-mechanical assumptions (1.4), closely tied to the presumed HLSP-PP-VB form of the wave function, that lead to persistent formal difficulties. Specifically, so that the wave function superposition (1.4a) leads to weighting factors (1.4b) satisfying (1.1b) (without the expected cross-terms), PW assumed the localized VB functions Ψ_α to be mutually orthogonal

$$\langle \Psi_\alpha \,|\, \Psi_\beta \rangle = \delta_{\alpha\beta}. \tag{2.1}$$

Moreover, so that the averaging property (1.1a) is satisfied for a general $\langle P \rangle = \langle \Psi | \hat{P} | \Psi \rangle$, it is evidently necessary that operator $\hat{P}$ have vanishing cross-terms between distinct valence-bond functions,

$$\langle \Psi_\alpha | \hat{P} | \Psi_\beta \rangle = \delta_{\alpha\beta} \langle P \rangle_\alpha. \tag{2.2}$$

Unfortunately, neither (2.1) nor (2.2) is generally valid for actual HLSP-PP-VB wave functions. Even when such constraints as (2.1) and (2.2) are ignored, *ab initio* evaluation of the wave function (1.4a) as a superposition of HLSP-PP-VB functions leads to disturbing inconsistencies with ''chemical intuition.''[16] For the classical case of benzene, for example, it was found[16a] that the weights of covalent Kekulé and Dewar structures are actually *smaller* than those of the ionic structures that are usually ignored as ''negligible.''

A further consequence of the PW assumptions is the proliferation of structures necessary to represent ''covalent-ionic resonance.'' Because the Heitler-London covalent *ansatz* is specific to homopolar bonds, it became necessary to add ''ionic'' VB functions (which actually have quite high overlap with the corresponding covalent functions[17]) to describe polar bonding. This contributed an unfortunate impression of extreme bonding ''types''[18] and necessitated use of multiple resonance structures for simple polar molecules (e.g., H_2O) that are expected to be well described by a single Lewis structure formula. In contrast, it was emphasized by Mulliken[19] that a polar bond σ_{AB} between bonding hybrids h_A and h_B could be well represented by a single bond-orbital function

$$\sigma_{AB} = c_A h_A + c_B h_B \tag{2.3}$$

with polarization coefficients c_A and c_B that vary smoothly between covalent and ionic limits. Such an MO viewpoint stresses the unified picture of polar covalence, allowing one to replace pairs of PW covalent-ionic resonance structures with a *single* localized bond-orbital function (e.g., of NBO form). As discussed in an accompanying paper, the polarization coefficients c_A and c_B of (2.3) can be used to infer the ''percentage ionic character'' if it is desired to make contact with bond orders and valencies in the older PW framework of covalent-ionic resonance.

Owing to such logical and numerical difficulties, the original PW formulation of resonance theory has been largely neglected for quantitative purposes. As Streitwieser[20] remarked, ''There can be no question but that the development of resonance theory had much heuristic value in stimulating thought, understanding, and research in organic chemistry. Nevertheless, the theory is essentially qualitative and intuitive and consequently has been misused frequently. Neither resonance theory nor its parent VB theory is suited for general quantitative or semiquantitative calculations and correlations.''

Density Matrix Theory of Resonance Averaging

As was noted above, the PW coherent superposition *ansatz* (1.4a) is generally inconsistent with the desired resonance-averaging property (1.1), owing to cross-terms that are not negligible. However, we may observe that the *necessary and sufficient* condition for the resonance-averaging condition (1.1) to hold for *any p*-electron property is that the *p*th-order reduced density operator[14] $\Gamma^{(p)}$ be expressible as a ''convex'' weighted combination of density operators $\hat{\Gamma}_\alpha^{(p)}$ for idealized localized structures,

$$\hat{\Gamma}^{(p)} = \sum_\alpha w_\alpha \hat{\Gamma}_\alpha^{(p)} \tag{3.1}$$

with weighting coefficients satisfying (1.1b). In contrast to the coherent wave function *ansatz* (1.4), the fundamental NRT expression (3.1) describes a resonance hybrid as an *incoherent* superposition of localized density matrices. Insofar as (3.1) is both necessary and sufficient for (1.1), it represents no new assumption but is merely a rigorous quantum-mechanical statement of the resonance-averaging hypothesis (1.1) for general *p*-particle properties. Moreover, the resonance-averaging hypothesis is most commonly applied to formal *one*-electron properties (such as charge distribution or molecular geometry[21]), governed by the *first*-order reduced density operator that suffices to describe Hartree-Fock MO theory. We therefore specialize to $p = 1$ and rewrite (3.1) in terms of the first-order reduced density operator $\hat{\Gamma}^{(1)} \equiv \hat{\Gamma}$

$$\hat{\Gamma} = N\int \Psi(1,2\ldots N)\Psi^*(1',2\ldots N)\,\mathrm{d}2\ldots\mathrm{d}N \tag{3.2}$$

as

$$\hat{\Gamma} = \sum_\alpha w_\alpha \hat{\Gamma}_\alpha. \tag{3.3}$$

The required normalization, hermiticity, and positivity properties[14] of $\hat{\Gamma}$ are preserved for positive, normalized weighting factors satisfying (1.1b).

Given the true density operator $\hat{\Gamma}$ and a set of candidate density operators for idealized localized resonance structures $\{\hat{\Gamma}_\alpha\}$, we can formulate the resonance-theoretic hypothesis (3.3) as a least-squares *variational functional* for the unknown weighting factors $\{w_\alpha\}$

$$\delta_{\underline{w}} = \min_{\{w_\alpha\}} \left\| \hat{\Gamma} - \sum_\alpha w_\alpha \hat{\Gamma}_\alpha \right\| \tag{3.4}$$

where

$$\| \hat{A}\| = \left[\sum_{i\le j} A_{ij}^2 \right]^{1/2} \tag{3.5}$$

denotes the matrix norm in a matrix representation $\{A_{ij}\}$ of operator $\hat{A}$. The variational ''error'' $\delta_{\underline{w}}$ evidently vanishes if, and only if, (3.3) is an *exact* representation of the true $\hat{\Gamma}$, i.e., if the resonance-theory hypothesis (1.1) is exactly satisfied for the system in question. Therefore, $\delta_{\underline{w}}$ is a measure of the irreducible error in describing $\hat{\Gamma}$ with the chosen resonance structures $\{\hat{\Gamma}_\alpha\}$, providing an *internal criterion of accuracy* of the resonance expansion (3.3).

Furthermore, if δ_{ref} denotes the corresponding quantity for a *single*-term expansion in which $\hat{\Gamma}$ is approximated by the leading ''reference'' structure $\hat{\Gamma}_{\mathrm{ref}}$

$$\delta_{\mathrm{ref}} = \|\hat{\Gamma} - \hat{\Gamma}_{\mathrm{ref}}\|, \tag{3.6}$$

one can express the accuracy of the resonance expansion in terms of the fractional improvement $f_{\underline{w}}$ of the resonance-weighted (3.3) with respect to a corresponding single-term localized representation,

$$f_{\underline{w}} = \frac{\delta_{\mathrm{ref}} - \delta_{\underline{w}}}{\delta_{\mathrm{ref}}}. \tag{3.7}$$

The resonance-weighted $f_{\underline{w}}$ evidently varies in the range

$$0 \le f_{\underline{w}} \le 1 \tag{3.8}$$

where $f_{\underline{w}} \to 1$ as (3.3) becomes *exact* (i.e., $\delta_{\underline{w}} = 0$), or $f_{\underline{w}} \to 0$ if the resonance weighting gives no improvement over a single-term localized repre-

sentation (i.e., $\delta_{\underline{w}} = \delta_{\text{ref}}$). The quantity $f_{\underline{w}}$ thus represents the fraction of the "delocalization error" that is recovered by the resonance expansion (3.3) with weights $\underline{w}$, where

$$\max_{\{w_\alpha\}} f_{\underline{w}} \to 1 \tag{3.9}$$

as the resonance-theoretic description becomes exact.[22]

Insofar as the one-particle density operator $\hat{\Gamma}$ can be used to define NBOs of an idealized natural Lewis structure and the associated density operator $\hat{\Gamma}_\alpha$ (see the following section), (3.3)–(3.9) lead to an *ab initio* NBO-based algorithm to evaluate a set of optimal resonance weights $\{w_\alpha\}$ based solely on the information contained in $\hat{\Gamma}$. We describe this "natural" resonance theory (NRT) algorithm in the following section.

NRT Theory

NBO SELECTION OF CANDIDATE STRUCTURES AND CONSTRUCTION OF ASSOCIATED DENSITY MATRICES

The NBO analysis program[23] can be used to obtain the various resonance structures and associated density matrices $\hat{\Gamma}_\alpha$ discussed above. Given a molecular wave function Ψ of arbitrary form or accuracy, it is now a routine task to extract the optimal natural bond orbitals $\{\Omega_i\}$ for an optimal Lewis-type wave function $\Psi^{(L)}$. For a closed-shell system,[24] this is of the form

$$\Psi^{(L)} = \det\left|(\Omega_1)^2(\Omega_2)^2 \cdots\right| \tag{4.1}$$

where the Ω_i are doubly occupied NBOs representing localized electron-pair bonds or lone pairs of the formal Lewis structure. The $N/2$-occupied NBOs $\{\Omega_i\}$ are complemented by the residual set of non-Lewis (antibond and Rydberg) NBOs $\{\Omega_j^*\}$ that complete the span of the basis. Nonzero occupancies q_j^* of the latter orbitals

$$q_j^* = \langle \Omega_j^* | \hat{\Gamma} | \Omega_j^* \rangle \tag{4.2}$$

correspond to delocalization, i.e., departures of the true Ψ from the idealized Lewis-structure form $\Psi^{(L)}$. Numerous applications of the NBO algorithm have established that the NBO Lewis structures are generally in excellent agreement with the corresponding classical Lewis structures and bond hybridization concepts of elementary valence theory.[15]

The NBO program routinely provides information on the individual $\Omega_i \to \Omega_j^*$ NBO interactions that lead to breakdown of the localized $\Psi^{(L)}$ representation of the wave function, i.e., that lead to nonzero q_j^*s. The interaction between a Lewis-type A—B bond NBO (σ_{AB}) and a non-Lewis C—D antibond NBO (σ_{CD}^*) can be represented schematically as a "two-electron stabilizing interaction" with mnemonic diagram

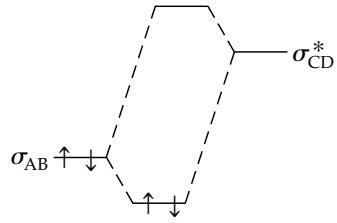

Each such interaction can be expressed in the language of resonance theory as a correction due to an additional resonance structure. For example, if atoms A, B, C, D are bonded as shown below in the parent resonance structure III, the $\sigma_{AB} \to \sigma_{CD}^*$ NBO interaction can be pictured in terms of the alternate resonance structures IV and V, shown below.

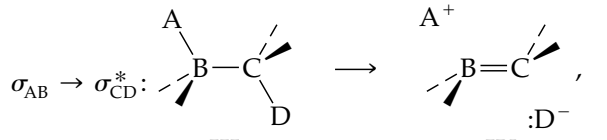

III **IV**

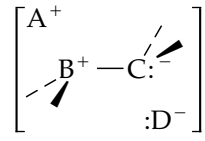

V (4.3)

Here, the doubly ionic form V (the direct result of transferring an electron pair from σ_{AB} to σ_{CD}^*) is reducible to the "double bond–no bond" form IV by B—C electron-pair sharing to cancel adjacent formal charges; that is, the "covalent-ionic resonance" pair IV ↔ V is reduced to the *single* Lewis structure IV with polarized B—C bond. Thus, one expects that a strong NBO interaction $\sigma_{AB} \to \sigma_{CD}^*$ is associated with reduced weight w_{III} of the parent structure III and increased weight w_{IV} of the secondary structure IV.

In a similar manner, a *delocalization list* of $\Omega_i \to \Omega_j^*$ NBO interactions of a parent reference structure can be used to generate a list of the associated

secondary structures describing the delocalized resonance hybrid. The list of resonance structures included in (3.3) will thus be closely tied to the entries of the NBO delocalization list, each resonance structure α being uniquely associated with a particular $\Omega_i \rightarrow \Omega_j^*$ NBO interaction. In Hartree-Fock theory, the importance of a particular $\Omega_i \rightarrow \Omega_j^*$ interaction can be judged from the second-order perturbation theory estimate of the stabilizing energy of interaction, viz.,

$$\Delta E^{(2)} = 2\frac{\langle \sigma_{AB}|\hat{F}|\sigma_{CD}^*\rangle^2}{\Delta\epsilon} \qquad (4.4a)$$

where

$$\Delta\epsilon = \langle \sigma_{CD}^*|\hat{F}|\sigma_{CD}^*\rangle - \langle \sigma_{AB}|\hat{F}|\sigma_{AB}\rangle \qquad (4.4b)$$

and $\hat{F}$ is the Fock operator. The delocalization list of leading NBO interactions and second-order stabilization energies (4.4a) is routinely included in the NBO program output for molecular orbital wave functions. [In the case of correlated wave functions, where no Fock operator is available, we use the approximate proportionality between $\hat{F}$ and $\hat{\Gamma}$ to generate a list of leading $\Omega_i \rightarrow \Omega_j^*$ interactions from a function of density matrix elements analogous to (4.4).] By selecting an energetic (or density matrix) threshold to control the number of entries in the delocalization list, one can control the number of resonance structures in the resonance expansion. Each resonance structure generated in this manner thus serves as a mnemonic for one of the $\Omega_i \rightarrow \Omega_j^*$ NBO interactions of the standard delocalization list.

Given the formal resonance structure formula, one can use the NBO program to calculate the optimal set of NBOs for this structure (CHOOSE option).[23] From the wave function analogous to (4.1) having these NBOs doubly occupied, one readily constructs the idealized density matrix for the resonance structure. Note that, in the most direct implementation of (3.4), the determination of a complete set of NBOs would be required for each candidate resonance structure.

The NRT program (see Appendix A) can sample a wide variety of candidate structures. An initial list of candidate structures can be generated from the delocalization list of the standard NBO Lewis structure. However, other candidate structures can be 1) generated (in subroutine LEWIS) from the Wiberg bond index,[25] 2) generated from the delocalization lists for any previous list of candidate structures, or 3) specified by the user. In particular, option 2 can generate many additional candidate structures in an iterative cycle. Options 1–3 guarantee that large numbers of possible candidate structures are generated and tested for their contribution to (3.4), leading to a computationally intensive task. We therefore examine special limiting cases to simplify the generation and assessment of candidate resonance structures.

WEAK DELOCALIZATION "SINGLE REFERENCE" LIMIT

When a single NBO Lewis structure is dominant and electron delocalization is weak, an important simplification of (3.4) is possible. It is then convenient to represent all secondary density matrices $\hat{\Gamma}_\alpha$ (and $\hat{\Gamma}$ itself) in the basis set of NBOs of the parent NBO structure. In this limit, the density matrix $\hat{\Gamma}$ is strongly dominated by its diagonal elements (NBO "populations"), and the deviations from locality can be conveniently expressed in terms of the diagonal NBO population shifts alone. (The more general case is considered in the next section.)

Let $\{\Omega_k\}$ represent the *fixed set* of NBOs of both Lewis and non-Lewis type for a fixed parent resonance structure of the system. For the actual wave function Ψ, associated with the one-particle density operator (3.2), the NBO occupancies q_k,

$$q_k = \langle \Omega_k|\hat{\Gamma}|\Omega_k\rangle, \qquad (4.5)$$

reflect the actual delocalization pattern. We denote by $\tilde{q}_k$ the corresponding quantity for the resonance-weighted density operator [cf. (3.3)],

$$\tilde{q}_k = \langle \Omega_k|\sum_\alpha w_\alpha \hat{\Gamma}_\alpha|\Omega_k\rangle. \qquad (4.6)$$

In place of minimization (3.4) with respect to the full matrix norm (3.5), we now consider the corresponding minimization with respect to diagonal elements alone,

$$d(\underline{w}) = \min_{\{w_\alpha\}}\left[\frac{1}{n_{bas}}\sum_k (q_k - \tilde{q}_k)^2\right]^{1/2}. \qquad (4.7)$$

The effectiveness of the variational criterion (4.7) can be assessed with respect to the limiting value $d(0)$ for a *single* resonance structure ($w_1 = 1$, $w_2 = w_3 = \cdots = 0$), expressed as the fractional improvement $f(\underline{w})$, analogous to (3.7),

$$f(\underline{w}) = \frac{d(0) - d(\underline{w})}{d(0)}. \qquad (4.8)$$

Compared to the full minimization (3.4), the restricted diagonal functional (4.7) allows one to expand significantly the list of resonance structures to be considered, incorporating a broader range of delocalization effects. It is therefore convenient to use this simplified procedure to determine the relative weightings of a manifold of secondary structures associated with the parent reference structure, the composite set forming a ''reference manifold.'' As shown in the numerical examples of the companion papers the variational optimization of (4.7) can be carried out without practical difficulties for hundreds of candidate secondary structures, whereas that involving (3.4) is restricted to a small number of structures, owing to storage and cpu-time limitations. A composite strategy that takes advantage of the simplified variational functional (4.7) is sketched below under Composite NRT Algorithm.

To streamline further the generation of candidate resonance density matrices, we restrict these matrices to preserve the forms of NBOs for electron pairs that are not rearranged with respect to the parent structure. The steps to form the modified NBOs and density operator $\hat{\Gamma}_\alpha$ for an idealized resonance structure α can be outlined as follows, using the example of (4.3): In terms of constituent natural atomic hybrids, we may write σ_{AB} as a bond composed from hybrids h_A and h_B and σ^*_{CD} as an antibond composed from hybrids h_C and h_D.

$$\sigma_{AB} = c_A h_A + c_B h_B \tag{4.9a}$$

$$\sigma^*_{CD} = c_D h_C - c_C h_D \tag{4.9b}$$

The schematic diagram (4.3) expresses the fact that the doubly occupied NBOs $(\sigma_{AB})^2(\sigma_{CD})^2$ of the parent structure III are to be replaced by doubly occupied NBOs $(\pi_{BC})^2(h_D)^2$ in structure IV, where the form of the new bond (say, π_{BC}) between h_B and h_C should be chosen to have the maximal occupancy (''natural'') property in the new electronic arrangement. This construction is carried out using the 4×4 density matrix block $\underline{\underline{\Gamma}}^{(4\times4)}$ in the basis of natural hybrid orbitals (NHOs),

$$\underline{\underline{\Gamma}}^{(4\times4)} = \begin{pmatrix} \gamma_{AA} & \gamma_{AB} & \gamma_{AC} & \gamma_{AD} \\ \gamma_{AB} & \gamma_{BB} & \gamma_{BC} & \gamma_{BD} \\ \gamma_{AC} & \gamma_{BC} & \gamma_{CC} & \gamma_{CD} \\ \gamma_{AD} & \gamma_{BD} & \gamma_{CD} & \gamma_{DD} \end{pmatrix} \tag{4.10}$$

where $\gamma_{AB} = \langle h_A|\hat{\Gamma}|h_B\rangle$, etc. To simulate the electron redistribution associated with $\sigma_{AB} \rightarrow \sigma^*_{CD}$, we first redistribute the occupancy q_{AB} of σ_{AB} into h_C and h_D in proportion to the polarization coefficients of the antibond σ^*_{CD} on each center. Specifically, the original occupancy of hybrid h_B stems from its proportionate share of the occupancy of bond σ_{AB} $(c_B^2 q_{AB})$ plus antibond σ^*_{AB} $(c_A^2 q^*_{AB})$, but the former contribution is now transferred to σ^*_{CD} and apportioned between hybrids h_C and h_D. We then diagonalize the 2×2 block associated with h_B and h_C,

$$\underline{\underline{\Gamma}}^{(2\times2)} = \begin{pmatrix} c_A^2 q^*_{AB} & \gamma_{BC} \\ \gamma_{BC} & \gamma_{CC} + c_D^2 q_{AB} \end{pmatrix}, \tag{4.11}$$

to find the optimal form of the new bond (π_{BC}) between h_B and h_C. The density matrix $\hat{\Gamma}_\alpha$ corresponding to the $(\pi_{BC})^2(h_D)^2$ configuration can then be constructed from these modified NBOs, all other NBOs having the fixed form of the parent structure. The steps (4.9)–(4.11) give a density matrix $\hat{\Gamma}_\alpha$ conforming to the specific $\sigma_{AB} \rightarrow \sigma^*_{CD}$ NBO interaction from which the resonance structure originates. Because the modified resonance structures $\hat{\Gamma}_\alpha$ differ from the parent structure only in blocks of small dimension, the required transformations can be carried out efficiently.

In the single-reference limit, the stabilization energy ΔE_α associated with each secondary structure α can be related to a particular NBO donor–acceptor interaction and estimated by second-order perturbation theory. Standard second-order arguments[26] demonstrate that the energy lowering $\Delta E_\alpha = \Delta E_{i \rightarrow j^*}$ associated with charge transfer from donor NBO Ω_i to acceptor NBO Ω^*_j is approximately proportional to q^*_j, the quantity of charge transferred,

$$q^*_j \cong (\text{const}) \cdot \Delta E_{i \rightarrow j^*} \tag{4.12}$$

where the proportionality constant is of order *unity* when both q^*_j and ΔE_α are expressed in atomic units. This limit allows one to recognize how the NRT formalism leads to the characteristic relationship (1.3) between resonance stabilization and resonance weighting; in the limit that the occupancy of Ω^*_j is entirely due to the $\Omega_i \rightarrow \Omega^*_j$ delocalization, (4.6) reduces to a single term,

$$q^*_j \simeq w_\alpha \langle \Omega^*_j|\hat{\Gamma}_\alpha|\Omega^*_j\rangle, \tag{4.13}$$

and Ω^*_j is doubly occupied in the charge-transferred structure α,

$$\langle \Omega^*_j|\hat{\Gamma}_\alpha|\Omega^*_j\rangle \simeq 2. \tag{4.14}$$

Equations (4.12)–(4.14) lead to a proportionality of the form

$$w_{i \to j^*} \propto \Delta E_{i \to j^*}, \qquad (4.15)$$

which can be compared with (1.3). Such considerations show why the NRT resonance weights must be qualitatively consistent with empirical postulates of electromerism/resonance theory.

STRONG DELOCALIZATION "MULTIREFERENCE" LIMIT

In cases where delocalization effects are so strong that no single NBO Lewis structure is dominant, it is necessary to consider the off-diagonal density matrix elements as incorporated in (3.4). In effect, stronger delocalization effects bring in off-diagonal *distortions* of bonding hybrids and NBOs as well as diagonal population shifts. For this limit we must consider *multiple* reference structures, as in the well-known example of benzene, in which the two leading Kekulé structures are equivalent. If $\{\hat{\Gamma}^{(r)}\}$ denotes a selected set of reference structures with resonance weights $\{W^{(r)}\}$, we can consider the variational functional $D(\underline{W})$, analogous to (3.4),

$$D(\underline{W}) = \min_{\{W^{(r)}\}} \left\| \hat{\Gamma} - \sum_r W^{(r)} \hat{\Gamma}^{(r)} \right\| \qquad (4.16)$$

and the associated fractional accuracy $F(\underline{W})$, analogous to (3.7),

$$F(\underline{W}) = \frac{D(0) - D(\underline{W})}{D(0)}, \qquad (4.17)$$

where $D(0)$ is the difference (4.13) for a chosen single-term expansion.

The limit in which *all* resonance structures are treated equivalently in the full variational functional (4.16) rapidly becomes an intractable numerical problem, particularly for large aromatic systems. The following difficulties arise.

1. Because no resonance structure has primacy, we must determine a full set of optimal NBOs for each resonance structure (analogous to the CHOOSE option), instead of only the two NBOs differing from a reference structure. This implies that the density matrices $\hat{\Gamma}^{(r)}$ differ from one another by a transformation of full dimension, rather than the 2×2 transforms of the weak delocalization limit.

2. In general, there is no single set of hybrids or NBOs, as in the weak delocalization limit, to serve conveniently as a common basis for the density matrices required in (4.16). However, the natural atomic orbitals (NAOs)[26] provide a common "democratic" basis set to form matrix representations of the $\hat{\Gamma}^{(r)}$'s. In the program, the density matrix for each $\hat{\Gamma}^{(r)}$ is initially formed in terms of its own NBOs, then transformed to the common NAO basis before performing the resonance averaging of (4.16).

3. The variational minimization of (4.16) becomes computationally intensive and slowly convergent as the number and dimensionality of resonance density matrices increase. However, because resonance structure diagrams are intrinsically restricted to *valence* bonds, we may omit the contributions of core and Rydberg orbitals, restricting our attention to the valence subspace. This significantly reduces the dimensionality and improves the numerical stability of the variational problem (4.16) in extended basis sets, affecting both storage and cpu time. In the program, the valence NBOs of each resonance structure are projected onto the valence NAO space, then symmetrically reorthogonalized before transforming the valence block of each $\hat{\Gamma}^{(r)}$ to the common NAO basis.

In light of these difficulties (as well as the greater cpu demands of the simulated annealing algorithm employed for multireference optimization; see below), our program is presently restricted to a maximum of 100 resonance structures for full multireference averaging. Whereas a full multireference treatment based on (4.16) is a more democratic treatment of delocalization effects, the severe limitation on the number of structures would have the undesirable effect of restricting attention to only the most important delocalizations, losing details of the NBO delocalization list. We are therefore led to consider an alternative approach, which combines the benefits of weak and strong delocalization limits.

COMPOSITE NRT ALGORITHM

As a practical compromise, we adopted a composite NRT algorithm that combines aspects of the weak and strong delocalization limits. The iterative NRT algorithm has the following steps:

1. Choose a provisional initial set of n_{ref} reference structures r.

2. Carry out a complete NBO analysis of Ψ for each reference structure $\hat{\Gamma}^{(r)}$ and use the associated delocalization list to generate a manifold of secondary structures $\hat{\Gamma}_\alpha^{(r)}$ for each reference structure (controlled by the NRTTHR threshold; see Appendix B).

3. Use the ''weak delocalization'' procedure (see above) to find resonance weights $w_\alpha^{(r)}$ for each manifold by minimizing $d(\underline{W}^{(r)})$ of (4.11).

4. Use the ''strong delocalization'' procedure (see previous section) to find resonance weights $W^{(r)}$ for the n_{ref} reference structures by minimizing the $D(\underline{W})$ functional of (4.16).

5. Calculate the composite weight w_α of each distinct structure (primary or secondary) as an average of its values in the various reference manifolds, weighted by the overall $W^{(r)}$ of the manifold.

$$w_\alpha = \sum_r^{n_{ref}} W^{(r)} w_\alpha^{(r)} \qquad (4.18)$$

6. Scan the list of structures for any structure whose weight w_α exceeds the preset threshold NRTWGT (default 35%; see Appendix B) and append each to the list of reference structures. Also, delete from the reference list any structure of weight less than threshold.

7. If the reference list was modified in step 6, return to step 2; otherwise, stop.

[A special case occurs if a structure r lies close to the NRTWGT threshold weight, such that including the structure as a reference structure leads to $w_\alpha <$ NRTWGT (and removal from the reference list), but omitting it leads to $w_\alpha >$ NRTWGT (and reinstallation in the reference list). In this case, nonconvergent oscillations are avoided by storing $D(\underline{W})$ in each cycle, then terminating the algorithm for whichever set gives lower $D(\underline{W})$.]

Note that single-reference optimization (step 3) usually involves a larger number of unknown resonance weights than does multireference optimization (step 4), but the latter is typically the most compute-intensive step. Appendix B describes further details of the NRTTHR and NRTWGT thresholds that control the overall cycle.

Numerical Aspects of NRT Weighting

The unknown NRT resonance weights $\{w_\alpha\}$ are obtained by solving the nonlinear least-squares minimization problems (4.7) and (4.16) in an iterative cycle. Because the number of unknown w_αs generally bears no special relation to the number of input density matrix elements (determined by the number of NBOs, or the dimension of the orbital basis set), the possibility arises of nonunique or intermediate solutions, multiple minima, or other numerical difficulties. In this respect the variational functionals (4.7) and (4.16) present different difficulties and are treated by different numerical methods.

MULTIREFERENCE OPTIMIZATION

For multireference optimization (4.16), the number of unknowns $\{W^{(r)}\}$ is typically small compared to the number of input density matrix elements, and the variational surface exhibits a large number of local minima that complicate the search for the global minimum. To achieve the necessary global view of the $D(\underline{W})$ surface and reduce the dependence on initial guesses of the weights, we employed the *simulated annealing* (SA) algorithm.[27]

Briefly, the SA algorithm is based on a nested sequence of macro- and microiterations, involving controlled random walks on the $D(\underline{W})$ surface. Each macroiteration is associated with an effective ''temperature'' T_i (initially set to a high value), which governs the average size of the region sampled in the associated random walk (microiterations). For given T_i, this walk consists of steps (random changes in $W^{(r)}$s) generated by a Metropolis Monte Carlo algorithm, where each step tends to be rejected, with probability dictated by a temperature-dependent Boltzmann-like factor, if the move is energetically uphill, and to be accepted otherwise. The temperature T_i is gradually reduced, shortening the average excursions permitted on the random walk, as the procedure converges. Further details of our implementation of this algorithm are presented in Appendix B.

In practice, we find that the SA algorithm converges smoothly and efficiently to a unique solution that is independent of the initial guesses, random number seed, etc. This independence and robustness indicate that the minimization (4.16) is a reasonably well-behaved numerical problem for reasonable NRT expansion lengths.

SINGLE-REFERENCE OPTIMIZATION

As a more efficient method for solving the variational problem (4.7), we have adopted the analytic-gradient BFGS (Broyden-Fletcher-Goldfarb-Shanno) algorithm,[27] which employs a modified steepest-descent method. Analytic gradients of $d(\underline{w})$ (see Appendix B) were combined with Boltzmann-like initial estimates[28]

$$\tilde{w}_\alpha \propto e^{-3\rho_\alpha^*} \qquad (4.19)$$

(ρ_α^* = non-Lewis density of structure α) to give a rapidly convergent procedure that preserves in-

trinsic symmetries of the problem. The default BFGS solutions were checked against alternative SA solutions to verify accuracy and uniqueness for a wide variety of molecules and basis set levels, as described below. Our program checks for numerical indeterminancy or nonuniqueness by evaluating the eigenvalues of the analytic Hessian matrix and, if necessary, repeats the optimization with the SA algorithm, using a penalty function to select a unique solution. Additional details of the optimization strategy and numerical characteristics of the NRT program are given in Appendices A and B.

Conclusions

We have described a new ''natural'' resonance theory (NRT) algorithm for calculating resonance structures and resonance weights to describe electronic delocalization effects in molecules. As with the natural bond orbital (NBO) method on which it is based, the NRT method uses information contained in the first-order reduced density matrix and is therefore applicable to any *ab initio* or semiempirical wave function, density functional, or perturbation method for which a density matrix is available. The NRT resonance weighting is based on a variational criterion for a resonance-weighted approximation to the true density matrix. Although the theoretical assumptions underlying NRT differ significantly from those of classical Pauling-Wheland theory, we find that NRT results give qualitative agreement with key physical concepts of Pauling-Wheland theory (see the two companion papers). The NRT description is typically found to be of high quantitative accuracy, with the leading few structures often accounting for 80–90% of the delocalization density ''error'' (itself a very small fraction of the total electron density). Thus, NRT resonance weights give a reasonably quantitative description of the subtleties of electronic delocalization in a compact, chemically intuitive language.

Although the NRT description of delocalization is appealingly simple, it is somewhat less detailed than the NBO analysis from which it derives. This is seen most clearly in the case of delocalization involving core or Rydberg orbitals, which have no counterpart in the NRT framework (because resonance structures depict only *valence* bond reorganization). Another restriction arises when two or more NBO delocalizations correspond to the *same* resonance structure (e.g., the $n_N \rightarrow \sigma^*_{CO}$ and $n_N \rightarrow \pi^*_{CO}$ delocalizations of a twisted amide I, both of which would be depicted by a resonance structure of form II) masking physically distinct electronic effects. Nevertheless, the NRT expansion provides a mnemonic picture, complementary to NBO analysis, that allows the principal features of electronic delocalization to be grasped intuitively. The two companion papers describe NRT bond order and atomic valency indices and present detailed numerical applications to a variety of weakly and strongly delocalized chemical species.

Appendix A. The NRT Program

INTRODUCTION

The NRT program has been integrated into the standard NBO program,[23] which in turn can be linked into standard electronic structure packages such as Gaussian 9X, GAMESS, or Ampac. Familiarity with certain details of the NBO program will therefore be assumed in describing the NRT implementation. The present brief summary allows NRT program segments to be connected with their logical function and specific equations, options, or thresholds mentioned in the text.

The NRT program performs two basic functions: 1) generating a list of n_{RS} candidate resonance (Lewis) structures $\Psi^{(L)}_\alpha$ for the NRT expansion and 2) assigning resonance weights w_α based on the variational functionals (4.7) and (4.16). The first task is primarily implemented in subroutines LEWIS, KEKULE, CHOOSE, SHREWD, ARROWS, SECRES, and SUPPL, as described in the next section, and the second is implemented in subroutines BFGS, POWELL, ANNEAL, and MULTI as described below under Numerical Optimization of Resonance Weights. The final section of Appendix A describes the calculation of analytic derivatives of the variational functional (4.7).

GENERATION OF RESONANCE STRUCTURES

Given wave function Ψ, the NRT program constructs a list of one or more parent ''reference'' Lewis structures that describe the leading delocalization in the molecule. Subroutine LEWIS performs an initial search for structures that 1) satisfy the octet rule for each nonhydrogen atom, 2) restrict formal charge for each nonhydrogen atom (within the limits imposed by the NRTCHG keyword, default +1 for a neutral species), and 3)

correspond qualitatively to Ψ (as judged by the Wiberg-NAO bond indices[25] $b_{AB}^{(W)}$). LEWIS searches all possible assignments of one- and two-center NBOs among the atoms, constructing provisional structures having up to b_{max} bonds between atomic centers A and B if $b_{AB}^{(W)} \geq thresh$, where *thresh* is 0.3, 1.1, or 1.7 for $b_{max} = 1$, 2, or 3, respectively. These loose constraints are designed to generate all plausible reference structures without excessive overhead of unreasonable structures that are tested and subsequently rejected.

At this initial stage in the NRT analysis, each $\Psi_\alpha^{(L)}$ is simply represented as a skeletal pattern of valence lone pairs and bonds, stored in TOPO (''topological'') matrix form with elements

$$\text{TOPO(I, I)} = \text{number of lone pairs on center I} \tag{A.1a}$$

$$\text{TOPO(I, J)} = \text{number of bonds between centers I and J.} \tag{A.1b}$$

Thus, in terms of TOPO matrix elements, constraints 1–3 given above become (for neutral closed shell wave functions)

$$2\sum_{J} \text{TOPO(I, J)} = 8, \quad \text{each nonhydrogen atom I} \tag{A.2a}$$

$$\left|2 * \text{TOPO(I, I)} + \sum_{J \neq I} \text{TOPO(I, J)} - Z_I\right| \leq \text{NRTCHG} \tag{A.2b}$$

$$\text{TOPO(I, J)} \leq b_{max} \tag{A.2c}$$

where Z_I is the valence nuclear charge of atom I.

Each skeletal TOPO matrix generated by LEWIS (supplemented, if necessary, by the main NBO structure) is passed by subroutine PARENT to CHOOSE or SHREWD for determination of an optimal set of NBOs, $\{\Omega_i\}$, corresponding to the resonance structure $\Psi_\alpha^{(L)}$. The CHOOSE and SHREWD routines perform the directed NBO search for a stipulated pattern of bonds and lone pairs. As usual, this NBO search returns the non-Lewis density ρ_α^* and a list of the principal delocalization terms ($\Omega_i \rightarrow \Omega_j^*$) associated with the structure, controlled by a threshold value for the second-order energy lowering (default: 1.0 kcal mol^{-1}).

Occasionally one recognizes that several resonance structures having distinct electron configurations have *identical* TOPO matrices (i.e., identical patterns of bonds and lone pairs) These may be called ''iso-Lewis'' structures, to suggest their identical bond topology. A simple example is given by the carbon dioxide molecule, which is described by a pair of iso-Lewis parent structures, each corresponding to the $:\ddot{O}=C=\ddot{O}:$ Lewis structure representation. In this case, the central C atom participates in two orthogonal pi bonds (say, π_x, π_y) to oxygen atoms, each O having a pi-type lone pair (n_y, n_x) orthogonal to its own pi bond. Interchange of x and y yields the two possible electron configurations arising from this pattern. Subroutine CHOOSE has been modified to recognize such a situation and to step systematically through the various $\Psi_\alpha^{(L)}$ structures arising from a single TOPO matrix. The CHOOSE routine recognizes when NBOs can be chosen in two or more distinct ways around a given atomic center. All possible alternative bonding hybrids are examined whenever the NBO search is forced to choose a lone pair having occupancy less than 1.9 electrons, and all possible alternative bonds are examined whenever the search forces selection of bonds having less than 1.9 electrons. When this occurs, CHOOSE initially selects the NBOs of higher occupancy and returns with an index flag indicating that alternative choices are possible. By systematically incrementing the index variable, the calling program can guide CHOOSE successively through the alternative resonance structures until all possibilities are explored. The thresholds for such alternative iso-Lewis structures are deliberately chosen conservatively so that no plausible structure is overlooked at this stage.

From the resulting list of candidate parent structures, subroutine SELECT generally selects the parent structure that best represents (according to its non-Lewis density ρ_α^*) the molecular structure, as well as other structures within $0.6e$ of the lowest ρ_α^*. For example, for the naphthalene molecule (RHF/3-21G level), subroutine LEWIS initially returns four parent structures

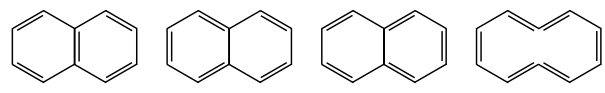

I **II** **III** **IV**

that adequately satisfy criteria 1–3 given above, and the CHOOSE search calculates respective non-Lewis densities of 1.8653, 2.2467, 2.2467, and 6.4998 electrons. Hence, only structures I–III

(within $0.6e$ of the minimal ρ_α^*) serve as candidate reference structures for the remainder of the NRT analysis, structure IV being discarded.

Secondary structures are generated by subroutine ARROWS, guided by the TOPO matrix and delocalization list of the reference structure. No attempt is made to generate a mathematically *complete* list of resonance structures (e.g., Rumer diagrams), because the vast majority of such structures would contribute negligibly. Instead, each $\Omega_i \rightarrow \Omega_j^*$ NBO interaction of the delocalization list is used to generate a single secondary TOPO matrix; cf. mnemonic (4.3). The total number of secondary resonance forms investigated is, therefore, effectively controlled by the user-selected energy threshold NRTTHR that determines the length of the delocalization list (and thus the level of detail) desired by the user. Subroutine CONDNS checks for redundancy between ionic structures with adjacent positive and negative formal charges and equivalent covalent forms, deleting the former if necessary. Subroutine KEKULE then searches for resonance structures that are related by concerted bond shifts (as in the two Kekulé structures of benzene). Such structures are appended to the secondary lists. Finally, the NBOs and delocalization density ρ_α^* of each secondary resonance form are calculated by subroutine SECRES, based on (4.9)–(4.11).

NUMERICAL OPTIMIZATION OF RESONANCE WEIGHTS

Having generated the structures of the resonance expansion, the NRT program performs a variational optimization, eqs. (4.7) and (4.16) of the NRT parameters. Three methods of optimization are provided by the NRT program, including steepest descent algorithms of Broyden-Fletcher-Goldfarb-Shanno and Powell (subroutines BFGS and POWELL) and a simulated annealing method (subroutine ANNEAL and MULTI). Due to restrictions eq. (1.1b), these algorithms optimize only $(n_{RS} - 1)$ resonance weights, the weight of the parent structure being determined by normalization, and the symmetry of the molecular system is retained by constraining symmetry-related resonance structures (as judged from the value of ρ_α^*) to have equivalent weights.

For a set of initial resonance weights, given by the exponential guess of (4.19), the steepest descent methods generally optimize to the nearest local minimum on the multidimensional $d(\underline{w})$ surface. Although there is nothing to guarantee that these methods achieve the *global* minimum of $d(\underline{w})$, we have found (through a wider exploration of the surface; see below) that this is usually the case when the exponential guesses are employed. For several reasons. a steepest descent method is, therefore, the method of choice for most NRT analyses. First, steepest descent methods are computationally efficient, particularly when analytic gradients are available (as with BFGS). Second, these methods automatically preserve the molecular symmetry of the problem to full numerical precision. Third, calculations on a wide variety of molecular systems have demonstrated that the weights computed by BFGS and POWELL do not differ significantly from those obtained from a more complete search of the $d(\underline{w})$ surface. Additional details of these algorithms are given by Press et al.[27] and Glendening.[28] For the purposes of the NRT program, numerical convergence of 10^{-6} and 10^{-5} [for $d(\underline{w})$] appears adequate for the BFGS and Powell algorithms, respectively. We have adopted BFGS as the default optimization procedure.

Alternatively, subroutine ANNEAL provides a more robust optimization algorithm (although at increased computational expense), which is particularly well-suited for locating the globally optimal resonance weights. In contrast to the task of the steepest descent methods, ANNEAL searches the closely related "$f(\underline{w})$ surface" [see (4.8)] for the global maximum. The NRT-simulated annealing algorithm consists of nested "macroiterations" and "microiterations," which control a random walk over the $f(\underline{w})$ surface. Each macroiteration (to a maximum of 500) has an associated temperature, T_i, and maximal step size, S_i, which govern acceptable walks taken during the microiterations. For the n_v variational parameters that define the configuration, up to $100n_v$ microiterations are taken at the given temperature. Each of these intermediate iterations is a three-step process: 1) a random change (up to $\pm S_i$) in one of the variational parameters, 2) evaluation of $f(\underline{w})$, and 3) conditional acceptance of the new configuration. The latter is based on the Metropolis algorithm, with the new configuration being unconditionally accepted if $f(\underline{w})$ increases during the walk, or with conditional probability

$$P_i = \exp[\Delta f(\underline{w})/T_i] \qquad \text{(A.3)}$$

otherwise. If the walk is unacceptable, the configuration is returned to its previous state. The annealing scheduler resets the temperature and step size

at each macrointeraction according to

$$T_{i+1} = 0.9 \cdot T_i \tag{A.4a}$$

$$S_{i+1} = 1.5 \cdot S_i^{(max)} \tag{A.4b}$$

where $S_i^{(max)}$ is the largest *accepted* step from the previous macroiteration. Macroiterations continue until both $f(\underline{w})$ and S_i are converged to 10^{-5} and $2 \cdot 10^{-5}$, respectively. This method of optimization is roughly two orders of magnitude more expensive than the steepest descent methods but is recommended when the results of the latter are suspect [e.g., when the $f(\underline{w})$ surface becomes particularly flat].

Numerically indeterminate (''flat'') surfaces are detected by checking for near-zero eigenvalues of the analytic Hessian (second-derivative) matrix. If a singular Hessian is detected for the default BFGS optimization, the optimization is automatically repeated using the SA algorithm with a penalty function included in $f(\underline{w})$ to select a unique solution having the most compact form. [Specifically, we maximize

$$\tilde{f}(\underline{w}) = f(\underline{w}) - \lambda\left(1 - \sum_\alpha w_\alpha^2\right)$$

with $\lambda = 0.001$.]

For multireference optimization, eq. (4.16), the SA algorithm of subroutine MULTI is used directly, analogous to that described above for single-reference optimization. Further details of the optimization procedures are described in the program documentation.

Subroutine SUPPL updates the list of reference structures after the optimizations are performed. A structure whose weight w_α [as determined by (4.18)] is at least 35% (NRTWGT) of that of the leading structure will be retained as a reference. Secondary forms of high weight are promoted to the reference list, and reference structures of low weight are deleted from it. SUPPL continues to iterate on the reference list, adding and deleting structures, until the resonance expansion converges or until oscillations are detected.

ANALYTIC DERIVATIVES OF THE VARIATIONAL FUNCTIONAL

The numerical efficiency of the BFGS algorithm relies, in part, on the availability of analytic derivatives of the variational functional, eq. (4.7). Differentiation with respect to a selected set of variational parameters $\{t_k\}$ leads to the expression

$$\frac{\partial d(\underline{w})}{\partial t_k} = \frac{1}{n \cdot d(\underline{w})} \sum_i \left(\sum_\alpha w_\alpha (q_{i\alpha} - q_i) \right) \cdot \left(\sum_\beta \frac{\partial w_\beta}{\partial t_k} (q_{i\beta} - q_i) \right) \tag{A.5}$$

where the outermost summation is over all n NBOs $\{\Omega_i\}$, and the qs are expectation values of the density operators $\hat{\Gamma}$ and $\hat{\Gamma}_\alpha$

$$q_i = \langle \Omega_i | \hat{\Gamma} | \Omega_i \rangle \tag{A.6a}$$

$$q_{i\alpha} = \langle \Omega_i | \hat{\Gamma}_\alpha | \Omega_i \rangle. \tag{A.6b}$$

Thus, given the relationship between the NRT weights $\{w_\alpha\}$ and the variational parameters, the calculation of analytic derivatives is relatively straightforward.

In BFGS (and also in POWELL) it is convenient to optimize the variational parameters $\{t_k\}$, which are related to the NRT weights $\{w_\alpha\}$ by

$$w_\alpha \propto \exp(-t_k). \tag{A.7}$$

This relationship has the desirable characteristic that, for any value t_k, the corresponding weight w_α is positive, as required by (1.1b). More explicitly, the NRT weights are given by the expression

$$w_\alpha = m_\alpha w_1 + \sum_k n_{\alpha k} \exp(-t_k) \tag{A.8}$$

where w_1 is the weight of the leading resonance structure (determined by normalization) and m_α and $n_{\alpha k}$ are pointers (ones and zeros) that map $\{w_\alpha\}$ onto w_1 and $\{t_k\}$. Note that, in general, several weights w_α will be mapped onto a single parameter t_k, thereby constraining symmetry-related resonance forms to have identical resonance weight. Differentiation of (A.8) under the normalization condition leads to

$$\frac{\partial w_\alpha}{\partial t_k} = \exp(-t_k)(m_\alpha g_k - n_{\alpha k}) \tag{A.9}$$

where

$$g_k = \frac{\Sigma_\alpha n_{\alpha k}}{\Sigma_\alpha m_\alpha}. \tag{A.10}$$

The calculation of analytic derivatives has been implemented in subroutine GETGRD.

Elements of the analytic Hessian (second-derivative) matrix

$$H_{\alpha\beta} = \frac{\partial^2 d(\underline{w})}{\partial w_\alpha \, \partial w_\beta} \qquad \text{(A.11)}$$

are evaluated by expressions analogous to (A.5)–(A.10). The Hessian matrix is considered to be singular if one or more eigenvalues fall below 10^{-9}. [As described above, in this case, the optimization is automatically repeated (using the SA algorithm) with an added penalty function to resolve the degeneracy of solutions.]

Appendix B. Numerical Accuracy of the Single-Reference NRT Description

To assess the numerical convergence, accuracy, and efficiency of the NRT description, we examined a set of 58 ''weakly delocalized'' molecules (Table I) with Pople-Gordon idealized geometry[29] for each species. These represent a broad cross section of acyclic neutral species involving up to three C, N, or O atoms for which a single reference structure should be adequate.

To test the stability of the NRT expansion with respect to improved levels of theory, we examined the full data set of molecules for three distinct basis set levels, 1) STO-3G (minimal basis), 2) 3-21G (split-valence double zeta), and 3) 6-31G* (double zeta plus polarization), all at the restricted Hartree-Fock (RHF) level of theory.[30] The minimal basis STO-3G level corresponds most nearly to the effective valence-shell basis of semiempirical VB-RT treatments, whereas the extended 6-31G* basis includes numerous functions to describe Rydberg (extra-valence-shell) interactions that have no counterpart in simple resonance theory. Table I exhibits the number of resonance structures (n_{RS}) and fractional improvement [$f(\underline{w})$] of the NRT expansion for all these species. For the 6-31G* basis set level, we have also included (column 7) the cpu computation time for NRT analysis (IBM RS/6000, model 580) and the total non-Lewis density (ρ^*) of the NBO reference structure. For example, for the first entry (C_2H_2O), in Table I, the RHF/6-31G* value $f(\underline{w}) = 0.9241$ means that the delocalization density ''error'' ($0.352e$) of the single-term NBO structure is reduced by approximately 92% (to $0.028e$) in the ten-term NRT expansion.

As is shown in Table I, the optimized NRT resonance expansions consistently describe the delocalization density with high percentage accuracy, approximately 95% at the STO-3G level and 80–85% at extended basis levels. Because these percentages refer to a quantity $d(0)$ that is itself a

TABLE I.
Number of Resonance Structures (n_{RS}) and Accuracy [$f(\underline{w})$] of the NRT Expansion for Various Molecules (All with Pople-Gordon Standard Geometries[25]) at Several *Ab Initio* RHF Basis Set Levels.[a]

	STO-3G		3-21G		6-31G*			
Molecule	n_{RS}	$f(\underline{w})$ (%)	n_{RS}	$f(\underline{w})$ (%)	n_{RS}	$f(\underline{w})$ (%)	t_{cpu} (s)	$\rho^*(e)$
1. C_2H_2O	8	97.97	12	93.57	10	92.41	33.8	0.352
2. C_2H_2O	9	97.68	10	93.50	10	93.13	32.0	0.162
3. C_2H_3N	7	94.73	12	94.80	12	93.34	38.9	0.210
4. C_2H_3N	12	98.64	14	94.61	14	92.23	33.7	0.234
5. C_2H_3N	10	94.54	13	64.02	10	64.54	18.3	0.119
6. C_2H_4O	21	99.02	17	93.58	14	91.12	10.6	0.165
7. C_2H_4O	15	97.66	10	78.65	10	82.22	33.0	0.153
8. C_2H_4	13	91.00	13	74.93	13	70.92	20.6	0.047
9. C_2H_5N	19	94.81	10	85.61	10	82.00	21.0	0.125
10. C_2H_5N	23	99.27	19	93.12	15	89.64	35.9	0.169
11. C_2H_5N	19	96.18	12	84.30	11	80.65	21.7	0.120
12. C_2H_6O	17	86.91	11	88.54	11	85.37	12.4	0.110
13. C_2H_6O	16	94.12	12	84.78	12	82.59	22.5	0.100
14. C_2H_6	7	89.36	7	72.94	7	77.31	22.9	0.046
15. C_2H_7N	23	97.84	15	88.12	15	84.10	24.5	0.112
16. C_2H_7N	21	97.61	14	84.32	14	81.22	24.8	0.101
17. C_3H_4	11	95.95	19	89.95	19	87.68	26.4	0.167

TABLE I.
(Continued)

Molecule	STO-3G		3-21G		6-31G*			
	n_{RS}	$f(\underline{w})$ (%)	n_{RS}	$f(\underline{w})$ (%)	n_{RS}	$f(\underline{w})$ (%)	t_{cpu} (s)	$\rho^*(e)$
18. C_3H_4	8	83.90	19	85.70	13	84.40	30.8	0.124
19. C_3H_6	19	84.29	19	80.88	19	78.24	41.7	0.107
20. C_3H_8	13	91.92	13	79.50	13	78.48	25.9	0.091
21. CH_2N_2	13	99.96	9	95.65	9	94.26	57.8	0.404
22. CH_2N_2	8	96.34	9	84.31	9	85.12	30.3	0.214
23. CH_2O_2	16	98.83	9	88.92	7	89.49	19.4	0.281
24. CH_2O	7	97.40	3	82.17	3	81.42	8.3	0.092
25. CH_3NO	17	98.41	9	87.10	9	88.21	9.5	0.262
26. CH_3NO	20	98.96	11	93.79	10	91.75	19.2	0.221
27. CH_3NO	17	99.40	10	93.19	9	89.05	28.4	0.145
28. CH_3NO	11	94.95	7	83.23	7	73.67	18.1	0.122
29. CH_3N	11	99.93	5	83.79	5	79.40	18.2	0.058
30. CH_4N_2	22	99.07	13	93.38	11	90.63	20.6	0.212
31. CH_4N_2	22	99.84	10	87.21	10	86.06	19.7	0.150
32. CH_4N_2	16	94.35	10	80.78	9	64.61	20.0	0.115
33. CH_4O_2	21	88.58	11	84.42	11	85.73	19.4	0.123
34. CH_4O_2	13	89.21	9	76.69	8	74.37	19.5	0.074
35. CH_4O	10	88.48	6	86.48	6	83.43	10.3	0.053
36. CH_5NO	18	96.86	11	85.53	10	78.57	11.6	0.101
37. CH_5NO	27	99.69	14	89.13	13	85.50	21.0	0.119
38. CH_5NO	19	96.22	12	83.77	11	75.69	21.5	0.100
39. CH_5N	15	99.74	8	86.16	8	82.63	21.0	0.055
40. CH_6N_2	29	99.78	17	88.85	15	84.07	23.0	0.118
41. CH_6N_2	24	94.22	11	81.33	11	73.85	22.3	0.094
42. CHNO	9	99.06	6	82.51	7	83.21	8.4	0.177
43. CHN	3	79.45	4	37.22	4	40.51	23.3	0.027
44. H_2N_2O	15	99.34	9	95.19	8	88.60	7.7	0.188
45. H_2N_2O	14	99.40	8	93.50	7	87.36	16.8	0.227
46. H_2N_2	9	99.91	5	79.79	5	59.67	17.9	0.049
47. H_2O_2	7	99.23	5	68.21	5	64.83	8.2	0.018
48. H_2O3	9	91.49	9	85.45	7	76.87	15.7	0.045
49. H_3N3	20	99.86	10	92.93	10	83.98	18.3	0.172
50. H_3NO_2	19	99.58	15	91.76	11	78.36	17.2	0.099
51. H_3NO_2	17	97.44	10	84.32	9	74.61	22.3	0.075
52. H_3NO	12	99.70	7	83.56	7	80.18	8.9	0.056
53. H_4N_2O	19	88.97	11	75.79	9	68.98	9.8	0.096
54. H_4N_2O	24	99.75	13	85.83	10	76.26	18.7	0.105
55. H_4N_2	17	91.01	5	66.12	5	56.00	18.9	0.036
56. H_5N3	28	99.71	11	78.95	9	70.32	19.8	0.097
57. HNO_2	9	99.15	8	94.50	7	90.66	16.6	0.257
58. HNO	4	99.65	3	87.46	3	73.22	7.5	0.049
Average		95.80		84.55		80.39		
S.D.		4.81		9.60		10.20		

[a] For the 6-31G* basis set, we also show the computation time t_{cpu} (IBM RS / 6000, model 580, cpu seconds) and total non-Lewis density (ρ^*). Structural isomers of the same stoichiometry are not further distinguished (e.g., molecules 1 and 2 are ketene and hydroxyacetylene, respectively); contact the authors for further details on individual entries.

small fraction ($\sim 1\%$) of the total electron density, these $f(\underline{w})$ values correspond to a very accurate overall description of the electron density. It is noteworthy that the cases of lowest $f(\underline{w})$ generally correspond to smallest $d(0)$ or ρ^* values (e.g., the reference structure of HCN, entry 43 in Table I, already describes more than 99.8% of the electron density at all three basis set levels), so that the overall percentage accuracy of the NRT description is higher and more uniform than might be

suggested by the rather large variations (5–10% standard deviation) in the $f(\underline{w})$ values. Overall, we conclude that the NRT expansion gives a very satisfactory combination of accuracy and compactness, expressing principal details of electronic delocalization in compact graphical form. The slight overall decline in $f(\underline{w})$ from minimal (95%) to extended (80–85%) basis sets reflects the role of Rydberg-type delocalization, particularly important for lone pairs on N and O atoms, that are systematically omitted in the NRT expansion. This relatively small decline is consistent with the Pauling-Wheland assumption that electron delocalization effects outside the formal valence shell are negligible.

The practicality of the NRT method is indicated by the cpu times (column 7 in Table I), which are seen to be on the order of a few seconds for all these systems. The results shown in Table I were all obtained with default thresholds of the NRT program, specifically the 1.0 kcal mol^{-1} NRTTHR threshold for entries of the delocalization list. As is shown in Table I, this typically leads to NRT expansions of fewer than 10–20 terms. A decrease of this NRTTHR threshold would naturally result in increased n_{RS} and computation times, as well as increased $f(\underline{w})$ values, but there appears to be no practical difficulty in extending the NRT expansions to much higher order. On the other hand, much of the conceptual attractiveness of resonance theory is associated with its compactness in representing delocalization effects. By increasing the NRTTHR threshold somewhat (say, NRTTHR = 2 kcal mol^{-1}), one could get shorter expansions (n_{RS} = 2–5) that still describe the great majority of the delocalization density.

Acknowledgments

Jay K. Badenhoop provided invaluable assistance in determining program thresholds, carrying out the numerical applications, and preparing program documentation. We gratefully acknowledge a generous grant of equipment from the IBM Corporation and other computational support provided by NSF grant CHE-9007850.

References

1. L. Pauling, *Proc. R. Soc. London*, **A356**, 433 (1993).
2. L. Pauling and G. W. Wheland, *J. Chem. Phys.*, **1**, 362 (1933); G. W. Wheland and L. Pauling, *J. Am. Chem. Soc.*, **57**, 2086 (1935); see also reference 12.
3. L. Pauling, *Nature of the Chemical Bond*, 3rd ed., Cornell University Press, Ithaca, NY, 1960.
4. G. W. Wheland, *The Theory of Resonance and its Applications to Organic Chemistry*, Wiley, New York, 1955.
5. Pauling himself acknowledged the need for a more quantitative formulation of resonance theory. For example, he states (reference 3, p. 569, in a section entitled ''The Further Development and Application of the Concept of Resonance'') that ''The applications of the idea of resonance that have been made during the last thirty years are in the main qualitative in nature. This represents only the first step, which should be followed by more refined treatments with quantitative significance.''
6. Reference 3, p. 232.
7. L. Pauling, L. O. Brockway, and J. Y. Beach, *J. Am. Chem. Soc.*, **57**, 2705 (1935).
8. Pauling (reference 3, pp. 219–220) states that ''The theory of resonance is essentially a chemical theory (an empirical theory, obtained largely by induction from the results of chemical experiments). Classical structure theory was developed purely from chemical facts, without any help from physics. The theory of resonance was also well on its way toward formulation before quantum mechanics was discovered.''
9. J. W. Armit and R. Robinson, *J. Chem. Soc.*, **121**, 827 (1922); J. Allen, A. E. Oxford, and J. C. Smith, *J. Chem. Soc.*, **129**, 401 (1926); R. Robinson, *Outline of an Electrochemical* [*Electronic*] *Theory of the Course of Organic Reactions*; Institute of Chemistry of Great Britain and Ireland, London, 1932.
10. C. K. Ingold, *J. Chem. Soc.*, **121**, 1133 (1922); C. K. Ingold and E. H. Ingold, *J. Chem. Soc.*, **129**, 1310 (1926); C. K. Ingold, *J. Chem. Soc.*, **1933**, 1120 (1933).
11. For additional discussion of the historical background of resonance theory, see A. R. Todd and J. W. Cornforth, *Biogr. Mem. Fellows R. Soc. London*, **22**, 415 (1977) and references 1 and 3 (p. 184).
12. W. Heitler and F. London, *Z. Phys.*, **44**, 455 (1927); J. C. Slater, *Phys. Rev.*, **37**, 481 (1931), **38**, 1109 (1931); L. Pauling, *J. Am. Chem. Soc.*, **53**, 1367 (1931), **53**, 3225 (1932), **54**, 998, 3570, (1932).
13. A useful historical overview of VB/resonance concepts and applications is given by D. J. Klein and N. Trinajstic, *J. Chem. Ed.*, **67**, 633 (1990). For representative works pertaining to (a) projecting VB-type structures from MO or MO-CI wave functions or density matrices, (b) VB-mixing descriptions of reactivity and properties, (c) classical or self-consistent VB computational methods, or (d) graph-theoretic methods, see: (a) M. Craig and R. S. Berry, *J. Am. Chem. Soc.*, **89**, 2801 (1967); P. C. Hiberty and C. Leforestier, *J. Am. Chem. Soc.*, **100**, 2012 (1978); P. C. Hiberty and G. Ohanessian, *Int. J. Quant. Chem.*, **27**, 259 (1978); P. C. Hiberty, *Int. J. Quant. Chem.*, **19**, 259 (1981); S. S. Shaik, *J. Am. Chem. Soc.*, **103**, 3692 (1981); P. C. Hiberty and G. Ohanessian, *J. Am. Chem. Soc.*, **104**, 66 (1982); P. C. Hiberty, G. Ohanessian, and F. Delbecq, *J. Am. Chem. Soc.*, **107**, 3095 (1985); R. M. Parrondo, P. Karafiloglou, and E. Sánchez Marcos, *Int. J. Quantum Chem.*, **52**, 1127 (1994). (b) S. S. Shaik, H. B. Schlegel, and S. T. Wolfe, *Theoretical Aspects of Physical Organic Chemistry*, Wiley, New York, 1992; A. Pross, *Theoretical and Physical Principles of Organic Reactivity*, Wiley, New York, 1995; N. D. Epiotis, *Lecture Notes in Chemistry, Vol. 34*, American Chemical Society, New York, 1983; F.

Bernardi and M. A. Robb, *J. Am. Chem. Soc.*, **106**, 54 (1984); Y. Apeloig and D. Arad, *J. Am. Chem. Soc.*, **108**, 3241 (1986); P. W. Anderson, *Science*, **235**, 1196 (1987); F. Bernardi, A. Bottoni, M. Olivucci, A. Venturini, and M. A. Robb, *J. Chem. Soc. Faraday Trans.*, **90**, 1617 (1994). (c) G. A. Gallup, R. L. Vance, J. R. Collins, and J. M. Norbeck, *Adv. Quantum Chem.*, **16**, 229 (1982); D. L. Cooper, J. Gerratt, and M. Raimondi, *Nature*, **323**, 699 (1986), *Adv. Chem. Phys*, **69**, 319 (1987); F. W. Bobrowitz and W. A. Goddard, in H. F. Schaefer (ed.), *Methods of Electronic Structure Theory*, *Vol. 3*, Plenum, New York, 1977, p. 72; A. F. Voter and W. A. Goddard, *J. Am. Chem. Soc.*, **108**, 2830 (1986); J. H. Van Lanthe, J. Verbeek, and P. Pulay, *Mol. Phys.*, **73**, 1159 (1991). (d) S. J. Cyvin and I. Gutman, *Kekulé Structures in Benzenoid Hydrocarbons*, Springer, Berlin, 1988.

14. P.-O. Löwdin, *Phys. Rev.*, **97**, 1474 (1955); E. R. Davidson, *Reduced Density Matrices in Quantum Chemistry*, Academic, New York, 1976.
15. J. P. Foster and F. Weinhold, *J. Am. Chem. Soc.*, **102**, 7211 (1980); A. E. Reed and F. Weinhold, *J. Chem. Phys.*, **78**, 4066 (1983); F. Weinhold and J. Carpenter, in R. Naaman and Z. Vager (eds.), *The Structure of Small Molecules and Ions*, Plenum, New York, 1988; A. E. Reed, L. A. Curtiss, and F. Weinhold, *Chem. Rev.*, **88**, 899 (1988).
16. J. M. Norbeck and G. A. Gallup, *J. Am. Chem. Soc.*, **96**, 3386 (1974); P. A. Mills, and F. Weinhold, *University of Wisconsin Theoretical Chemistry Institute Report WIS-TCI-674*, University of Wisconsin, Madison, 1982; for an earlier critique of valance bond theory with orthogonal atomic orbitals, see R. McWeeny, *Proc. R. Soc. London*, **A223**, 63, 306 (1954).
17. J. Braunstein and W. T. Simpson, *J. Chem. Phys.*, **23**, 176 (1955).
18. Pauling (reference 3, pp. 64–68) acknowledges the continuous nature of the change in bond type from covalent to ionic, but states that ''the bond might be described as *resonating between the covalent extreme and the ionic extreme*'' [p. 66; Pauling's italics] and that ''whenever a question arises as to the properties expected for a covalent bond with partial ionic character, it is to be answered by consideration of the corresponding resonating structures'' (p. 67).
19. R. S. Mulliken, *J. Chem. Phys.*, **3**, 573 (1935); for discussion of advantages of a general polar covalent description over that based on extreme covalent and ionic bond types, see R. T. Sanderson, *Polar Covalence*, Academic, New York, 1983.
20. A. Streitwiesser, *Molecular Orbital Theory for Organic Chemists*, Wiley, New York, 1961, p. 26.
21. Mathematical proof that molecular geometry is formally a one-electron property is given by K. F. Freed, *Chem. Phys. Lett.*, **2** 255 (1968).
22. As defined above, the upper limit $f_{\underline{w}} = 1$ is unattainable, insofar as the $\delta_{\underline{w}}$ functional (3.4) also contains irreducible contributions from core and Rydberg NBOs (the latter becoming increasingly numerous in extended basis sets) whose effects are not represented in the framework of ''valance bond'' resonance structures. However, a related criterion $f_{\underline{w}}^{(\mathrm{val})}$ could be defined to include only the *valance-level* delocalizations that the resonance expansion (3.3) could hope to represent. In practice, the difference between $f_{\underline{w}}$ and $f_{\underline{w}}^{(\mathrm{val})}$ is usually small (reflecting the relative unimportance of nonvalence-shell delocalizations); so we use the more conservative $f_{\underline{w}}$ criterion to describe the accuracy of the NRT expansion.
23. E. D. Glendening, A. E. Reed, J. E. Carpenter, and F. Weinhold, *QCPE Bull*, **10**, 58 (1990); F. Weinhold, *NBO 4.0 Program Manual*, Theoretical Chemistry Institute, University of Wisconsin, Madison, 1996.
24. The generalization to treat open-shell species is based on the concept of ''different Lewis structures for different spins''; J. E. Carpenter and F. Weinhold, *J. Mol. Struct. Theochem.*, **169**, 41 (1988); see following paper.
25. K. B. Wiberg, *Tetrahedron*, **24**, 1083 (1968).
26. A. E. Reed, R. B. Weinstock and F. Weinhold, *J. Chem. Phys.*, **83**, 735 (1985).
27. W. H. Press, B. P. Glannery, S. A. Tenkolsky, and W. T. Vetterling, *Numerical Recipes*, Cambridge University Press, New York, 1988.
28. E. D. Glendening, Ph.D. Thesis; U. Wisconsin: Madison, 1991.
29. J. A. Pople and M. Gordon, *J. Am. Chem. Soc.*, **89**, 4253 (1967).
30. W. J. Hehre, I. Radom, P. v. R. Schleyer, and J. A. Pople, *Ab Initio Molecular Orbital Theory*, Wiley, New York, 1986; Wave function calculations were performed with *Gaussian 92*, *Revision A*: M. J. Frisch, G. W. Trucks, M. Head-Gordon, P. M. W. Gill, M. W. Wong, J. B. Foresman, B. G. Johnson, H. B. Schlegel, M. A. Robb, E. S. Repogle, R. Gomperts, J. L. Andres, K. Raghavachari, J. S. Binkley, C. Gonzalez, R. L. Martin, D. J. Fox, D. J. Defrees, J. Baker, J. J. P. Stewart, and J. A. Pople, *Gaussian 92, Revision A*, Gaussian, Inc., Pittsburgh, 1992.